Molecular examination of fracture toughness of amorphous polyesters as a function of copolymerization component

Shigeo Asai, Nobuhiro Okabe, Masao Sumita* and Keizo Miyasaka
Department of Organic and Polymeric Materials, Faculty of Engineering, Tokyo Institute of Technology, Ookayama 2-12-1, Meguro-ku, Tokyo 152, Japan
(Received 18 August 1990; accepted 5 September 1990)

The fracture energy and the impact energy were measured for random copolymers of terephthalic acid (TPA), isophthalic acid (IPA), diphenyl-2,2′-dicarbonic acid (DA) and cyclohexane-dimethanol (CHDM). The fracture energy suddenly decreased when the DA fraction (DA/(DA + TPA)) was increased from 20 to 30%. Also the impact energy increased with increase in DA fraction. The energy levels of the possible processes of deformation which contribute to the fracture energy were calculated and compared with experimental data.

(Keywords: fracture toughness; amorphous polyesters; copolymerization)

INTRODUCTION

Recently, high-strength and high-modulus polymers have been used in the field of structural materials. Besides high strength, high toughness is also required. Generally, entangled network structure, which is influenced by molecular structure, chain stiffness and chain tortuosity, is thought to have a great influence on fracture toughness and strength below the glass transition temperature (T_g) in glassy polymers.

In this paper, we used polyester random copolymers which have different copolymerization components and investigated the influence of the copolymerization components and the molecular structure on fracture toughness.

EXPERIMENTAL

Samples. Polyester random copolymers of terephthalic acid (TPA), isophthalic acid (IPA), diphenyl-2,2′-dicarbonic acid (DA) and cyclohexane-dimethanol (CHDM) were used. The monomer fractions in the samples are shown in *Table 1*. Films were compression moulded from each polymer under a pressure of 180 kg cm^{-2} using a hot press, followed by quenching in ice–water. The moulding temperatures were 320, 300, 275, 240 and 240°C for DA0, DA10, DA20, DA30 and DA40, respectively.

Density. The densities of moulded specimens were determined according to ASTM 1506-60T in an n-heptane/carbon tetrachloride linear gradient at 20°C.

Glass transition temperature. These measurements were conducted on a DuPont 910 differential scanning calorimeter at a heating rate of 20°C min^{-1}.

Molecular weights. Molecular weights were measured at a temperature of 230°C using a gel permeation chromatograph (SSC-VHT-GPC7000, Senshu Scientific Co. Ltd).

Plateau modulus and molecular weight between entanglements. The dependence of dynamic storage modulus (G') and loss modulus (G'') and loss tangent ($\tan\delta$) on frequency were measured at a temperature over the T_g of each sample using a Rheometrics dynamic spectrometer (RDS-11).

The plateau modulus (G_n^0) was determined as G' at a frequency where $\tan\delta$ is at its minimum in the plateau zone[1,2]. From the value of G_n^0, the molecular weight between entanglements (M_e) was calculated using:

$$G_n^0 = \frac{\rho RT}{M_e}\left(1 - 2\frac{M_e}{M_w}\right) \quad (1)$$

where ρ is density, R is the gas constant, T is absolute temperature defining G_n^0 and M_w is the weight average molecular weight.

Three-point bend test. Notches of 1, 2, 3 and 5 mm depths were introduced into 3 mm thick rectangular specimens using a 0.2 mm thick diamond-blade. The specimen geometry is shown schematically in *Figure 1a*. Three-point bending tests were conducted on an Instron machine at a crosshead speed of 0.4, 1 and 15 mm min^{-1} at temperatures of $T_g - 50$°C for each sample. Bending strength (σ_f) and bending modulus (E_f) were calculated

Table 1 Copolymerization components of samples

Sample	DA	TPA	IPA	CHDM
DA0	0	95	5	100
DA10	10	90	0	100
DA20	20	80	0	100
DA30	30	70	0	100
DA40	40	60	0	100

* To whom correspondence should be addressed

0032-3861/91/132400-06

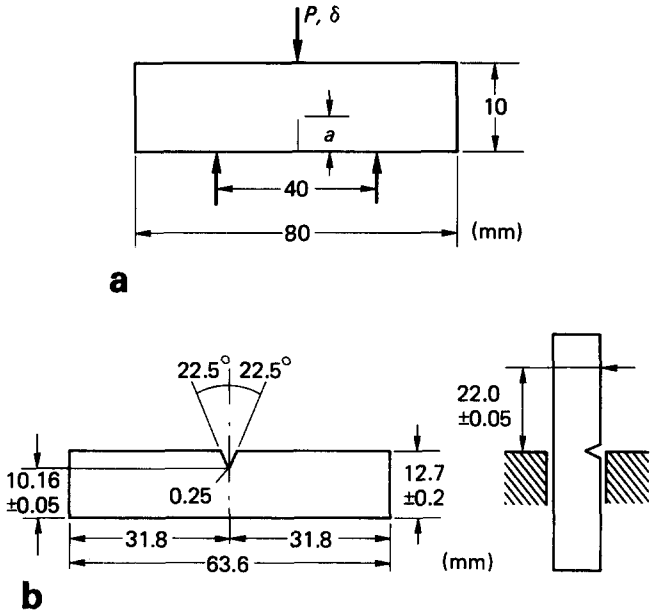

Figure 1 Specimen geometry: (a) three-point bend test; (b) Izod impact test

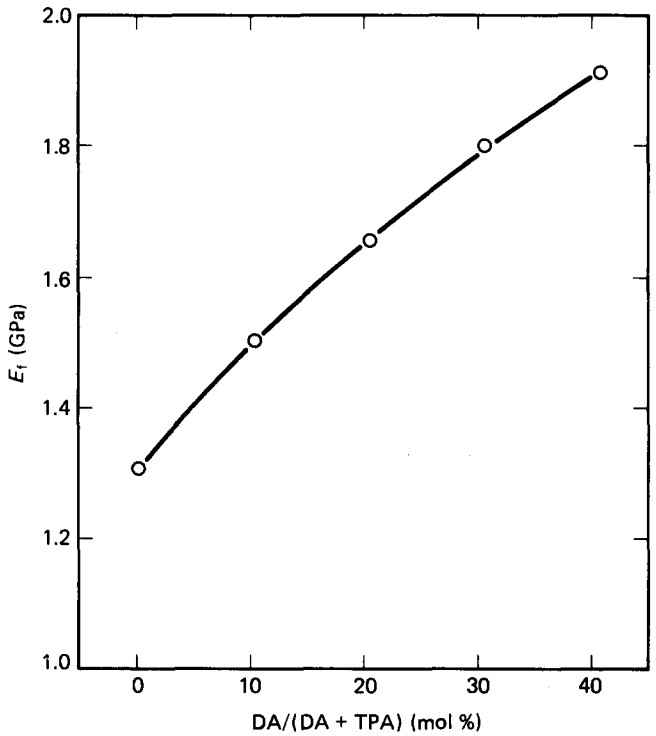

Figure 2 Modulus *versus* DA fraction

using:

$$\sigma_f = 3SP/2bh^2 \qquad E_f = S^3F/4bh^3d \qquad (2)$$

where P is the load which was determined according to ASTM-E399, S is the span, b is the width, h is the height, d is the displacement within the elastic limit and F is the load at d.

Izod impact test. A 22.5° angular notch of 2.54 mm depth was introduced into 3 mm thick rectangular specimens. The specimen geometry is shown schematically in *Figure 1b*. Izod impact tests were conducted on a Toyo Seiki Izod impact machine at an impact speed of ~1440 cm min^{-1} at a temperature of 23°C. The energy expended on the fracture surface of the specimen was divided by the thickness multiplied by the length of the ligament to determine fracture energy per unit area.

RESULTS AND DISCUSSION

Figures 2 and *3* show the bending modulus and strength, respectively, which were measured by the three-point bend test. They both increase with increase in DA fraction.

Figure 4 shows the bending strength of the notched samples *versus* the depth of the notch. According to linear fracture mechanics, the relationship between fracture

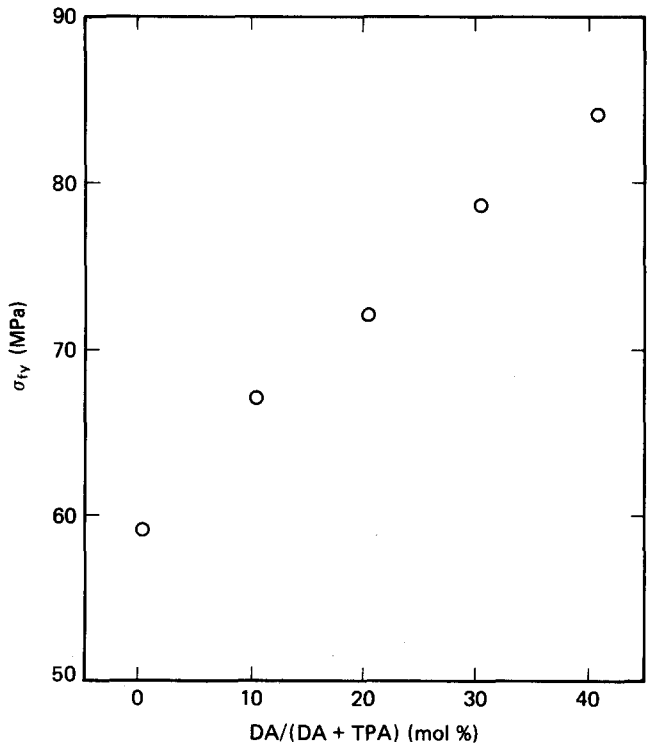

Figure 3 Strength *versus* DA fraction

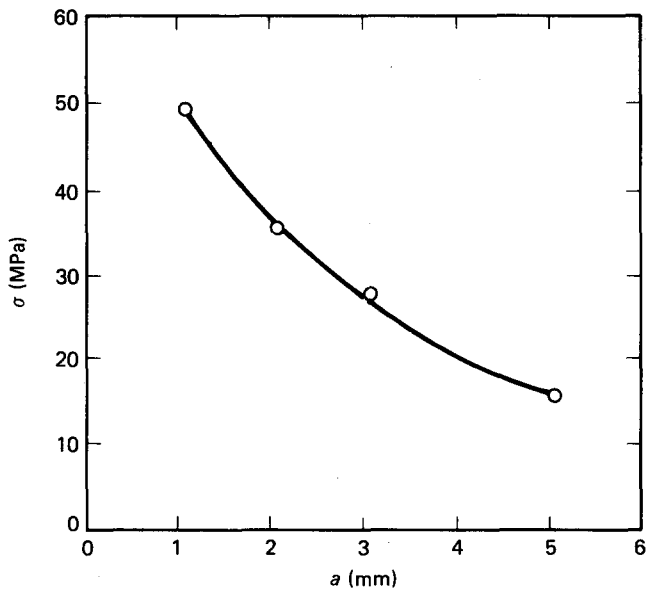

Figure 4 Typical plot of σ *versus* a

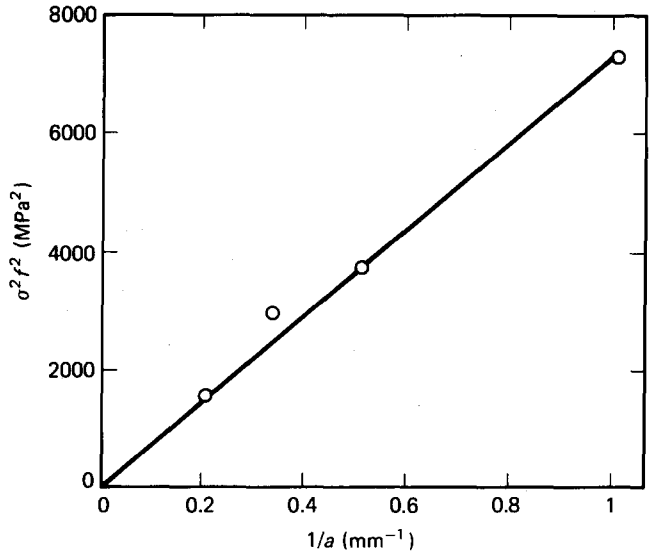

Figure 5 Typical plot of $\sigma^2 f^2$ *versus* $1/a$

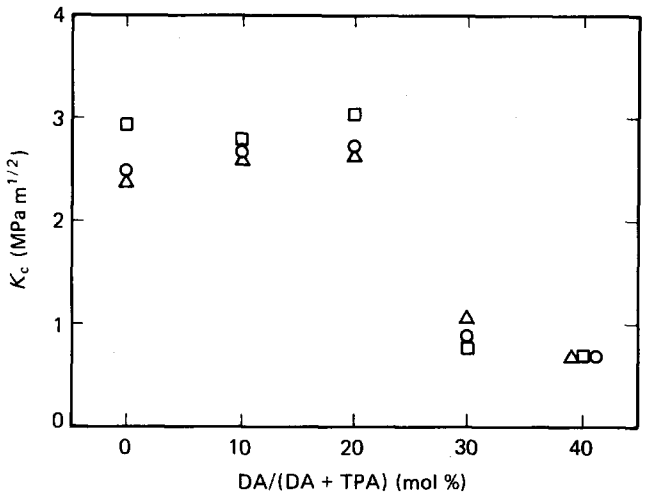

Figure 6 K_c *versus* DA fraction. Crosshead speed (mm min^{-1}): △, 0.4; ○, 1; □, 15

toughness (K_c), fracture strength (σ) and crack length (a) is:

$$K_c^2 = \sigma^2 f^2 a \tag{3}$$

where f is the stress concentration factor. When $S/h = 4$, f is expressed as[3]:

$$f = 1.93 - 3.07(a/h) + 14.53(a/h)^2 - 25.11(a/h)^3 + 25.8(a/h)^4 \tag{4}$$

Then K_c is determined from a plot of $\sigma^2 f^2$ *versus* $1/a$ (*Figure 5*).

Fracture energy (g_c) is expressed as:

$$g_c = K_c^2/E \tag{5}$$

where E is Young's modulus.

Figures 6 and *7* show K_c and g_c *versus* DA fraction. The value of K_c tends to increase slightly with increase in DA fraction until the DA fraction is 20%. The K_c of samples which have more than 30% DA fraction decreases dramatically. A similar trend is observed in the plot of g_c *versus* DA fraction.

Figure 8 shows scanning electron microscopy micrographs of the fracture surfaces of the 3 mm notched samples which were broken by the three-point bend test at a crosshead speed of 1 mm min^{-1}. The samples which have 0, 10 and 20% DA fraction have ductile behaviour but those which have 30 and 40% DA fraction have almost brittle behaviour.

It is surprising that g_c suddenly decreases when the DA fraction increases from 20 to 30%.

Figure 9 shows the result of the Izod impact test. Impact energy tends to increase with the increase in DA fraction.

On fracture of amorphous polymers in which molecules are entangled, the local plastic deformation occurs at the tip of the crack[4] and polymer chains extend across the crack surfaces. Then we consider the polymer chains extended across the crack surfaces and consider local chain extension, chain pull-out and chain scission as the possible processes of deformation which contribute to the fracture energy. The total fracture energy per polymer chain (e_t) can be expressed as[5]:

$$e_t = e_e + e_p + e_s \tag{6}$$

where e_e, e_p and e_s are the contributions due to local chain extension between entanglement points, chain pull-out from entanglement points and chain scission, respectively.

In order to estimate the contribution of each to g_c we model a polymer chain with an equivalent Kuhn chain. The Kuhn chain has the same chain contour length and end-to-end distance as a real chain. The Kuhn chain is defined by:

$$\langle R_2^0 \rangle = Nl^2 \tag{7}$$

$$L = n\langle l \rangle = Nl \tag{8}$$

where N is the number of Kuhn segments in a chain, l is the length of a Kuhn segment, $\langle R_0^2 \rangle$ is the mean-square end-to-end distance of a real chain and L is the chain contour length of a chain. Also, n is the number of real and/or virtual skeletal main chain bonds in a chain[2] and $\langle l \rangle$ is the average length of a real or virtual skeletal bond. We assume that the chain between entanglement points can be represented by the Kuhn chain:

$$d^2 = N_e l^2 \tag{9}$$

$$L_e = n_e\langle l \rangle = N_e l \tag{10}$$

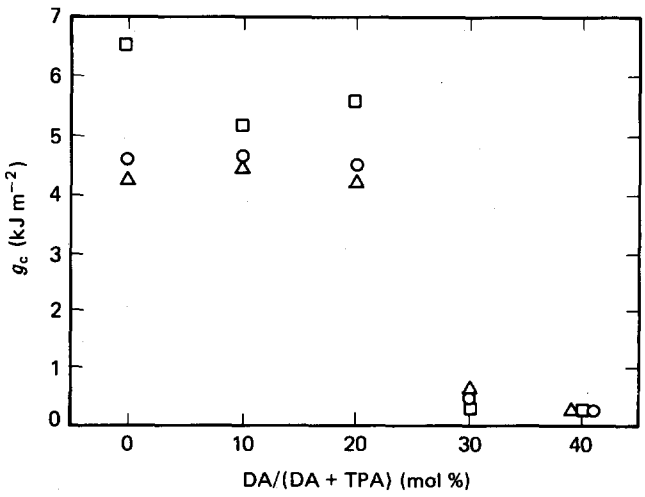

Figure 7 g_c *versus* DA fraction. Crosshead speed (mm min^{-1}): △, 0.4; ○, 1; □, 15

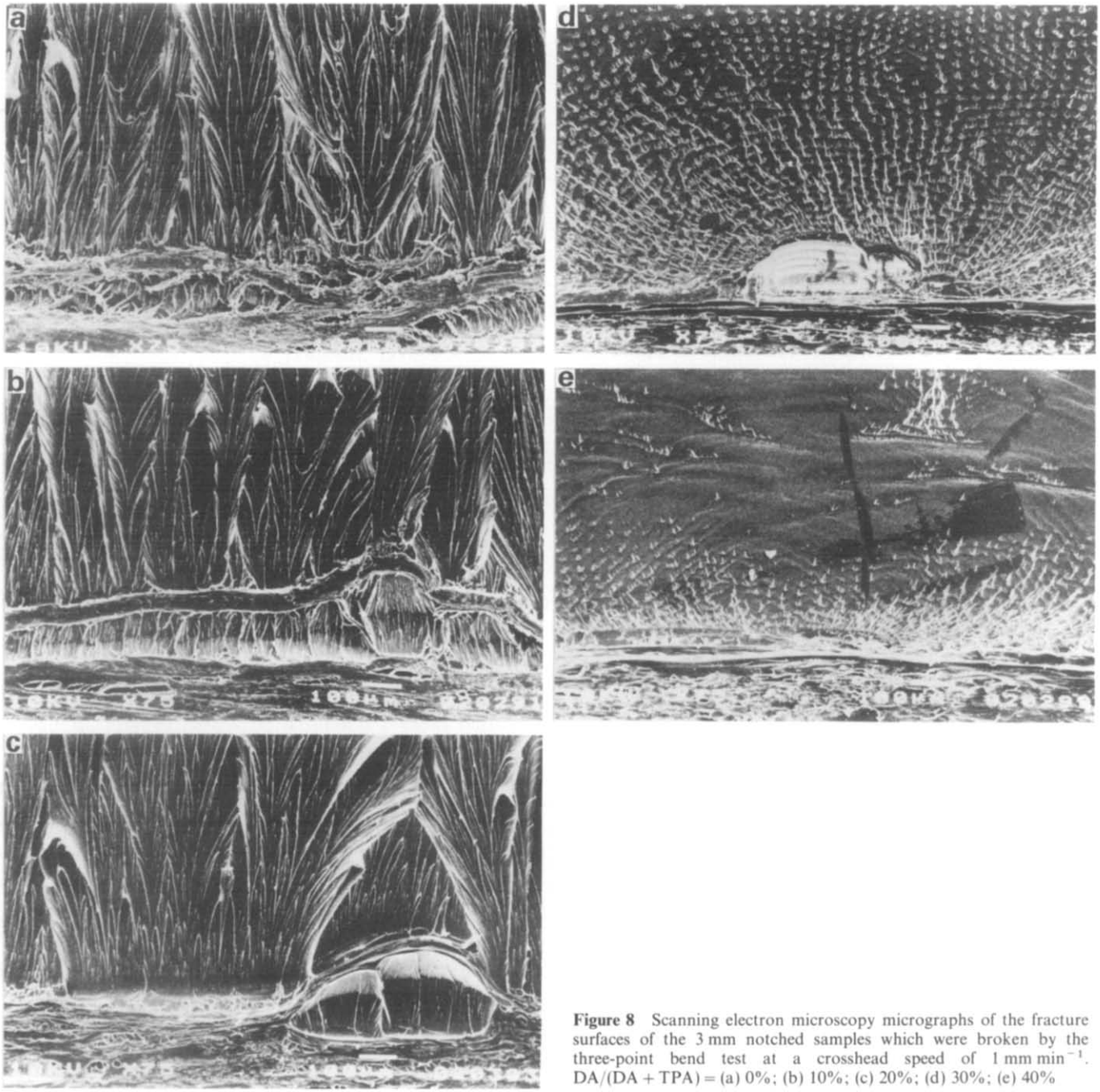

Figure 8 Scanning electron microscopy micrographs of the fracture surfaces of the 3 mm notched samples which were broken by the three-point bend test at a crosshead speed of 1 mm min^{-1}. DA/(DA + TPA) = (a) 0%; (b) 10%; (c) 20%; (d) 30%; (e) 40%

where d is an entanglement mesh size, L_e is the chain contour length of an entanglement strand, n_e is the number of real and/or virtual bonds in an entanglement strand[2] and N_e is the number of Kuhn segments in an entanglement strand. Using this model, we estimate the contribution of each factor in equation (10) by the classical theory of rubber elasticity[5,6].

When the chain between two entanglement points is fully extended, the energy absorption (e_e) is given by:

$$e_e = \int \frac{L_e}{d} \frac{3kT}{N_e l^2} r \, dr = \frac{3kT}{2} (N_e - 1) \qquad (11)$$

where k is Boltzmann's constant.

Next we consider the energy absorption by pulling the chain through entanglements (e_p). Suppose that, on application of a force F_p, the chain is pulled out of the tube with a velocity v. Then F_p is expressed by[6–8]:

$$F_p = \alpha v \qquad \alpha = kT/D_c \qquad (12)$$

where D_c is the curvilinear diffusion coefficient along the tube and α is the inverse of the mobility. In the reptation model, D_c is given by[7]:

$$D_c = D_1/N' \qquad (13)$$

where D_1 is the free diffusion constant of an individual segment, and N' is the number of segments in the tube. Hence:

$$F_p = kT \frac{N'}{D_1} v = \frac{kTv}{D_1 l} L' \qquad (14)$$

where L' is the tube length. Therefore:

$$e_p = \int_0^{L'} \frac{kTv}{D_1 l} x \, dx = \frac{kTv}{2D_1 l} L'^2 \qquad (15)$$

The chain length to be pulled through L' depends on the chain length and the velocity of chain pull-out, and it is not determined clearly. We estimate the energy absorption when the chain between two adjacent entanglements, whose length is $N_e l$, is pulled out until the length becomes the entanglement mesh size $d = N_e^{1/2} l$, then $L' = (N_e - N_e^{1/2})l$. In this case, e_p is given by:

$$e_p = \frac{kTv}{2D_1 l} l^2 (N_e - N_e^{1/2})^2 \tag{16}$$

According to Evans[5], when the velocity is low enough that chain scission does not occur, v and D_1 are given by:

$$v \sim l/\tau_1 \qquad D_1 \sim l^2/\tau_1 \tag{17}$$

where τ_1 is the molecular timescale for diffusion. Therefore, in this case:

$$e_p = (kT/2)(N_e - N_e^{1/2})^2 \tag{18}$$

The energy absorption by chain scission (e_s) will be sufficient to assume a value of the order of kT in this model. The value of kT is much smaller than the bond energy of C–O or C–C. Therefore, the purpose of these calculations of the fracture energy by this model is not to estimate the absolute value but to know the relative contribution of each to the process of deformation.

To know the fracture energy per unit area, we must know how many entanglements are involved per unit area. Assuming the entanglement points are distributed at random through space, the number of entanglements involved in the fracture surface of unit area is given by

$$n_{ep} = (\rho N_a / M_e)^{2/3} \tag{19}$$

where N_a is Avogadro's number. The energy absorption by local chain extension, chain pull-out and chain scission per unit area is then:

$$E_e = \left(\frac{\rho N_a}{M_e}\right)^{2/3} \frac{3kT}{2} (N_e - 1) \tag{20}$$

$$E_p = \left(\frac{\rho N_a}{M_e}\right)^{2/3} \frac{kT}{2} (N_e - N_e^{1/2})^2 \tag{21}$$

$$E_s = \left(\frac{\rho N_a}{M_e}\right)^{2/3} kT \tag{22}$$

To determine the value of N_e, we must know $\langle R_0^2 \rangle$ or C_∞, where C_∞ is the characteristic ratio and is defined by:

$$C_\infty = \langle R_0^2 \rangle / n \langle l^2 \rangle \tag{23}$$

where $\langle l^2 \rangle$ is the mean-square length of a real or virtual skeletal bond. However, C_∞ for our samples could not be determined by light scattering because the molecular weight was not large enough. We determined C_∞ using Wu's equation, $n_e = 3C_\infty^2$, which has been verified with experimental data for many polymers[2]. Therefore:

$$N_e = n_e / C_\infty = (3n_e)^{1/2} \tag{24}$$

$$n_e = M_e / \langle w \rangle \tag{25}$$

where $\langle w \rangle$ is the average molecular weight of a real or virtual skeletal bond. *Table 2* gives experimental data and chain parameters.

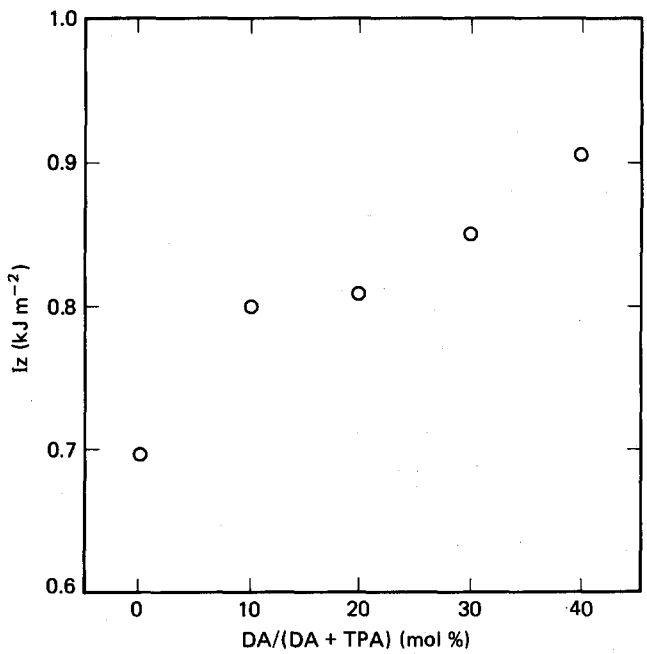

Figure 9 Impact energy *versus* DA fraction

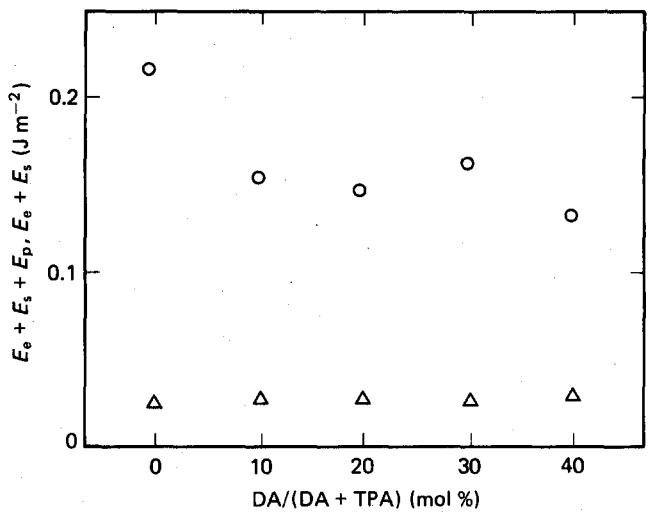

Figure 10 Energy absorption by the possible processes of deformation calculated from equations (20)–(22) *versus* DA fraction. ○, $E_e + E_s + E_p$; △, $E_e + E_s$

Table 2 Experimental data and chain parameters

Sample	DA/(DA + TPA) (%)	ρ (g cm^{-2})	M_w	G_n^0 (N m^{-2})	T (K)	M_e	n_e	C_∞	N_e
DA0	0	1.210	62200	1.024E + 5	388	17130	375	11	34
DA10	10	1.218	24300	2.212E + 5	383	7180	153	7	21
DA20	20	1.227	28400	3.182E + 5	378	6540	136	7	20
DA30	30	1.254	24500	1.139E + 5	378	9050	183	8	23
DA40	40	1.277	16500	2.644E + 5	373	5320	105	6	18

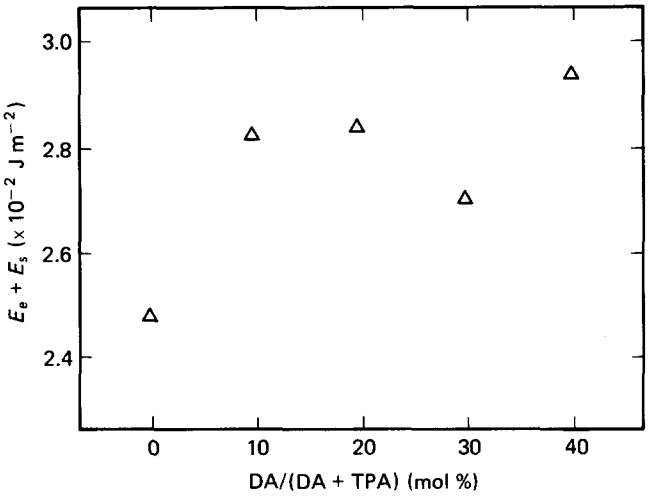

Figure 11 $E_e + E_s$ *versus* DA fraction

Figure 10 shows the energy absorption by the possible processes of deformation calculated from equations (20)–(22) *versus* DA fraction. Equations (20)–(22) involve some assumptions but it is found that the value of $E_e + E_p + E_s$ is much larger than that of $E_e + E_s$. In other words, the total energy absorption largely increases when chain pull-out occurs. From *Figures 7* and *10*, we believe that the origin of the large value for g_c in DA0, DA10 and DA20 is chain pull-out. In our sample we suggest that DA has the effect of preventing chain pull-out because of its bulky structure.

Figure 11 shows $E_e + E_s$ *versus* DA fraction; $E_e + E_s$ tends to increase with increase in DA fraction, which corresponds generally to the results of the Izod impact test in *Figure 9*. We conclude that in those cases where the crack growth rate is slow, chain pull-out does not occur, and the number of entanglements involved in the fracture surface of the unit area increases with the increase in DA fraction.

ACKNOWLEDGEMENT

The authors wish to express their gratitude to Toray Co. for providing samples.

REFERENCES

1 Wu, S. *J. Polym. Sci., Polym. Phys. Edn* 1987, **25**, 353
2 Wu, S. *J. Polym. Sci., Polym. Phys. Edn* 1989, **27**, 723
3 Brown, W. F. and Srawley, J. E. ASTM STP 410 1, 1966
4 Kramer, E. J. *Adv. Polym. Sci.* 1983, **52/53**, 1
5 Evans, K. E. *J. Polym. Sci., Polym. Phys. Edn* 1987, **25**, 353
6 Prentice, P. *Polymer* 1983, **24**, 344
7 Doi, M. and Edwards, S. F. *J. Chem. Soc. Faraday 2* 1978, **74**, 1789, 1802, 1818
8 Klein, J. *Contemp. Phys.* 1979, **20**, 611